*Korean J. Chem. Eng.*, **29**(1), 18-24 (2012)
DOI: 10.1007/s11814-011-0132-3

# Modeling of the non-catalytic semi-batch esterification of palm fatty acid distillate (PFAD)

**Seok Won Hong*, Hyun Jun Cho*, Soo Hyun Kim**, and Yeong Koo Yeo*,†**

*Department of Chemical Engineering, Hanyang University, Seoul 133-791, Korea
**Chemicals R&D Center, SK Chemicals, Bundang-gu, Seongnam-si, Gyeonggi-do 463-400, Korea
(*Received 28 February 2011 • accepted 11 May 2011*)

**Abstract**–Biodiesel fuel is one of the most attractive alternatives to the traditional diesel fuel derived from a petroleum refinery. Development of a reliable model for the biodiesel production process requires maximizing economics and enhancing safety in the commercial operation of biodiesel plants. We propose a model which represents effectively the non-catalytic biodiesel production reaction. In the modeling of the reaction, we employ a nonlinear programming scheme to estimate reaction kinetic parameters which minimize a specified objective function. The behavior of the methanol during the reaction is investigated both experimentally and numerically. Imperfect mixing in the liquid phase at the initial reaction stage causes a little discrepancy between the experimental data and results of simulations. Overall, the proposed model represents the biodiesel production reaction effectively.

Key words: Kinetics, Non-catalyst, Free Fatty Acids, Methyl Esterification, Semi-batch System

## INTRODUCTION

Recently, biodiesel has received much attention as one of the most attractive alternatives to the traditional diesel fuel derived from a petroleum refinery, especially by considering the recent steep increase in the petroleum cost [1]. Since biomass is used as raw material in the production of biodiesel fuel, biodiesel is considered as one of the most promising sustainable energy not causing exhaustion of natural resources. Moreover, biodiesel has little effect on environmental contamination because it has little toxicity and high biodegradability due to negligible content of sulfur and aromatics. Biodiesel, or more specifically free fatty acid ester, is currently produced by transesterification reaction based on animal fat or vegetable oils. However, crude oil almost always contains high amount of free fatty acids (FFAs), and the presence of too high FFAs easily results in soap formation during the transesterification reaction with alkali catalyst [2]. Thus, for commercial implementation without undesirable environmental effects, a novel process is required to recover FFAs from raw materials in addition to a process which separates soap products created by remnant FFAs, thus lowering the economics of the commercial production of the biodiesel. Recently, it was found that use of refined oil lowers the production cost of FFAs because additional separation processes for byproducts are not required. This reaction scheme has been paid much attention due to many advantages aforementioned.

In the esterification reaction represented by Eq. (1), long chain acids such as FFAs are reacted with short chain alcohols to give free fatty acid methyl ester (FAME) and water.

$$R-COOH+CH_3OH \rightarrow R-COO-CH_3+H_2O \quad (1)$$

Reaction products consisting of FAME and water are hydrolyzed to give reactants, and reaction (1) becomes a reversible reaction. In the reverse reaction, it takes too much time to achieve desired yield at atmospheric pressure and ambient temperature without addition of any other assistant materials. Therefore, it is natural practice to try catalytic reaction to attain fast reaction with high yield. Initially, homogeneous acids such as the sulfuric acid were used as catalysts. But acid catalysts are difficult to recover and large amount of water is consumed during the acid separation process from reaction products. Moreover, corrosion of reaction equipment is accompanied to increase overall operation production cost. As an alternative, the use of heterogeneous catalysts having branched acid group such as the sulfonic acid was proposed. A resin such as $SO_2ZrO_2$ can be used as a typical heterogeneous catalyst [3]. Use of heterogeneous catalysts makes separation and recovery relatively easy to overcome drawbacks of homogeneous catalysts. But, in general, heterogeneous catalysts do not exhibit enough stability at the reaction temperature and are more expensive compared to homogeneous catalysts.

To overcome these drawbacks, a non-catalytic esterification reaction scheme was proposed in which the reaction temperature and the pressure are changed and the methanol in supercritical state is used. The supercritical methanol maintains significant solubility, and characteristics of viscosity, diffusion and heat conductivity of it are similar to gases. It exhibits acidity without addition of any additives [4]. But relatively high pressure (more than 81 bar) has to be maintained during the reaction using supercritical methanol, and thus it can hardly be commercialized due to the high operation cost.

For the precise prediction of commercial production cost of biodiesel, we have to identify reaction kinetics more accurately. Diasakou et al. proposed kinetics of non-catalytic transesterification reaction of soybean oil [5]. In their three-step reaction kinetics, triglyceride, diglyceride and monoglyceride consisting raw material (crude oil) react with methanol to produce diglyceride, monoglyceride, glycerol and FAME respectively and reversible reactions were ignored. Joelianingsih et al. determined kinetic parameters based on non-catalytic transesterification experiments performed at atmospheric pressure [6]. Berrios et al. studied kinetics of esterification reactions of FFAs in sunflower oil [7]. In their experiments, the amount of homogeneous acid catalysts, the ratio of FFA to the methanol

†To whom correspondence should be addressed.
E-mail: ykyeo@hanyang.ac.kr

and the reaction temperature were key manipulating variables, and the forward reaction was modeled as 1st-order reaction while the reverse one was modeled as 2nd-order reaction. Tesser et al. investigated experimentally the reaction of oleic acid using heterogeneous sulfonic ion exchange resin catalyst, and their results were used as the basis of identification of reaction kinetics according to reactor types [1,8].

In the present work, we investigate the biodiesel production reaction performed in the semi-batch reactor at 230-290 °C and 8.5 bar, which are relatively lower than those employed in the reaction using supercritical methanol. For the modeling of the reaction, experimental data concerning changes of concentrations with respect to reaction time are used.

## EXPERIMENTAL

The palm fatty acid distillate (PFAD) used in experiments originated from Malaysia and was purchased from Sandakan Edible Oils SDN, BHD. The fatty acid (FFA) content of the PFAD is 87.3% and the rest of the PFAD is residue such as triglyceride which does not participate in the reaction. The oleic acid and the methyl oleate are considered as the key components of the FFA and the FAME, respectively, simply because of relatively larger amount than other components.

Fig. 1 shows the experimental apparatus designed for the isothermal and isobaric semi-batch system. At first, the semi-batch reactor (1) is charged with the reactants, PFAD, followed by introduction of the pure methanol via the feed pump (2) located at the bottom of the reactor. The impeller (3) reduces the formation of bubbles and disperses the generated bubbles within the liquid phase in the reactor. The main objective of the reactor controller (4) is to keep the internal temperature and RPM of the impeller as specified constant values by manipulating both the external electrical jacket (5) and the motor (6), respectively. The excess methanol, water produced during the reaction and little amount of FFA and FAME components which are vaporized and dispersed within the liquid phase are condensed in the condenser (7) and collected in the receiver (8). Sampling is performed through the sampling line (13) at a specified time interval. The sample is passed through the cooler (14) and is cooled rapidly well below 50 °C. Otherwise, methanol and water can be flashed because of their low boiling points.

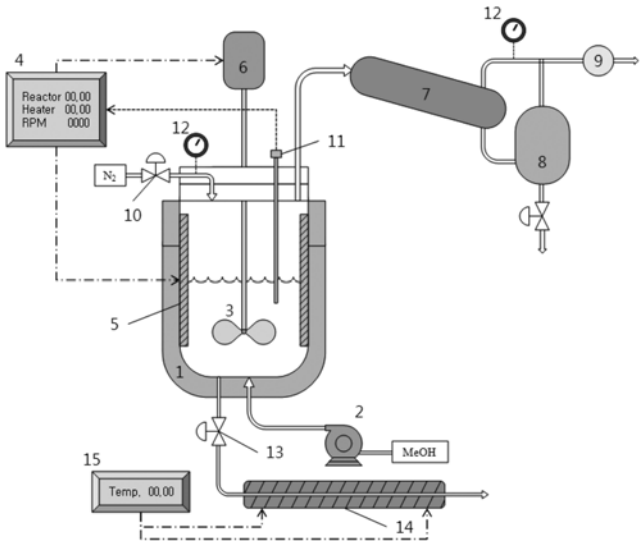


**Fig. 1. Schematic diagram of the experimental set-up.**

1. Semi-batch reactor (volume: 2 L)
2. Methanol feed pump
3. Impeller
4. Temperature and RPM controller
5. Electrical heater jacket
6. Motor
7. Condenser
8. Receiver
9. Pressure regulator
10. Nitrogen charging line
11. Thermocouple
12. Pressure gauge
13. Sampling line
14. Cooler (double jacketed)
15. Chiller

In the present work, the nitrogen gas is injected after specific amount of the PFAD (860 g) is charged into the reactor in order to pressurize the reactor up to the desired pressure. When the temperature of the reactor rises to the specific reaction temperature, methanol is fed into the reactor. The reactor temperature and speed of the impeller are maintained constant during the reaction. The reaction is terminated when the target reaction time is reached.

## MODELING DESCRIPTION

In this study, modeling is based on mass balances for liquid and gas phases in the well-stirred slurry reactor described by Santaesria et al. [7]. But their reaction was performed at 100-115 °C and 1 bar using heterogeneous resin catalysts. To model the pseudo-homogeneous reaction as a perfectly mixed non-catalytic reaction, it is obvious that some modifications are required. In the present reaction system, the oleic acid with constant concentration is reacted with methanol fed into the semi-batch reactor to produce FAME and water. The non-catalytic esterification reaction is considered to be a homogeneous phase equilibrium reaction and 1st-order kinetic is assumed for each component. Then the reaction rate can be written as

$$-r_A = -\frac{dC_A}{dt} = k_f C_A C_M - k_f C_E C_W \quad (2)$$

where $C_i$ denotes the concentration of component i and subscripts A, M, F and W represent fatty acid, methanol, fatty acid methyl ester and water, respectively. $k_f$ and $k_r$ are reaction constants for forward and reverse reaction, respectively. The reaction pressure is maintained at 8.5 bar while different reaction temperatures such as 230, 250, 270 and 290 °C are tested. Under these conditions, both FFA and FAME whose boiling points are relatively higher than specified reaction temperature remain in the liquid phase while the methanol and water with relatively low boiling points are vaporized. The amount of methanol reaches a certain steady-state level between the amount of continuously injected methanol and that of evaporated methanol. The water produced during the reaction is vaporized to cause the reaction equilibrium to be shifted to the right-hand side. Thus we can anticipate high yield from the reaction. The evaporation may be considered as the interfacial diffusion at the interface between vapor and liquid phases. Based on these observations, mass balances for the liquid can be given by

$$\frac{dn_{A,L}}{dt} = (-r_A V_L) \quad (3)$$

$$\frac{dn_{M,L}}{dt} = (-r_A V_L - J_M + F_L) \quad (4)$$

$$\frac{dn_{E,L}}{dt} = (r_A V_L) \quad (5)$$

$$\frac{dn_{W,L}}{dt} = (r_A V_L - J_W) \quad (6)$$

where $V_L$ is the liquid volume in the reactor, $F_L$ is the molar flow rate fed into the liquid phase and $J_i$ is the molar flow rate diffused from the liquid phase to the vapor phase. We assume that the methanol fed into the reactor is well stirred and mixed with liquid in the reactor. In PFAD, there are some residues which do not participate in the reaction and take part in a certain constant portion of the liquid phase. Mass balances for the vapor phase can be written as

$$\frac{dy_{N_2}}{dt} = -F_V(1 - y_M - y_W)\frac{1}{n_{T,V}} \quad (7)$$

$$\frac{dy_M}{dt} = (-F_V y_M + J_M)\frac{1}{n_{T,V}} \quad (8)$$

$$\frac{dy_W}{dt} = (-F_V y_W + J_W)\frac{1}{n_{T,V}} \quad (9)$$

where $F_V$ denotes the molar flow rate of vapor effluent from the upper part of the reactor and $n_{T,V}$ represents total number of moles existing in vapor phase. Since the reaction pressure is kept constant during the reaction, the value of $n_{T,V}$ is constant. At the initial reaction stage, the void part of the reactor (i.e., the volume of the reactor not occupied by the liquid phase) is filled with inert nitrogen gas to maintain constant pressure. As the reaction proceeds, water and methanol are evaporated and distributed evenly in the vapor phase. The amount of the mixed vapor discharged from the reactor is the same as that fed into the vapor phase from the liquid phase.

$$F_V = J_M + J_W \quad (10)$$

The volume of the solution may be assumed to be the sum of the liquid phase volume of each component and can be represented as Eq. (11).

$$V_L = \sum_i \frac{n_{i,L} MW_i}{\rho_i} \quad (11)$$

The volume of the vapor phase can easily be found by subtracting the liquid volume from the volume of the reactor. From the given temperature and pressure, the total number of moles of vapor phase can be computed by using an appropriate thermodynamic state equation. Fig. 2 represents a schematic of the semi-batch reactor with typical mass flows and reactions.

## RESULTS AND DISCUSSION

Most of the modeling studies presented so far are based on some assumptions that the amount of excess methanol is maintained constant and the reverse reaction is negligible. In other words, the rate of forward reaction is dependent only upon the concentration of FFA.

$$-r_A = k_f C_A C_M = k_f' C_A \quad (12)$$

The reaction rate (12), which is dependent only upon the concentration of FFA, cannot provide enough accuracy for actual plant design. Thus we need a more rigorous model to achieve enough accuracy for the model to be utilized in commercial plant design. From Fig. 3, we can see that the proposed model given by Eq. (2)-(11) exhibits better tracking performance to experimental data compared to the conventional model (Eq. (12)). As can be seen from Table 2, significant decrease in RMSEs for the mole fraction of FFA and FAME demonstrates superiority of the proposed model over the simple model. The proposed model incorporates reverse reactions

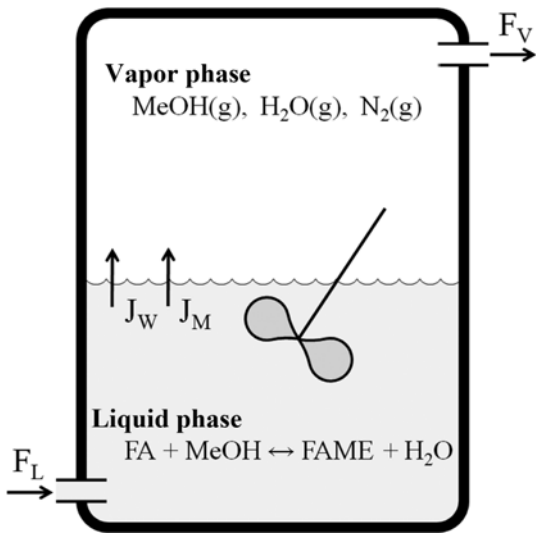


**Fig. 2. Simplified main flow in the semi-batch reactor.**

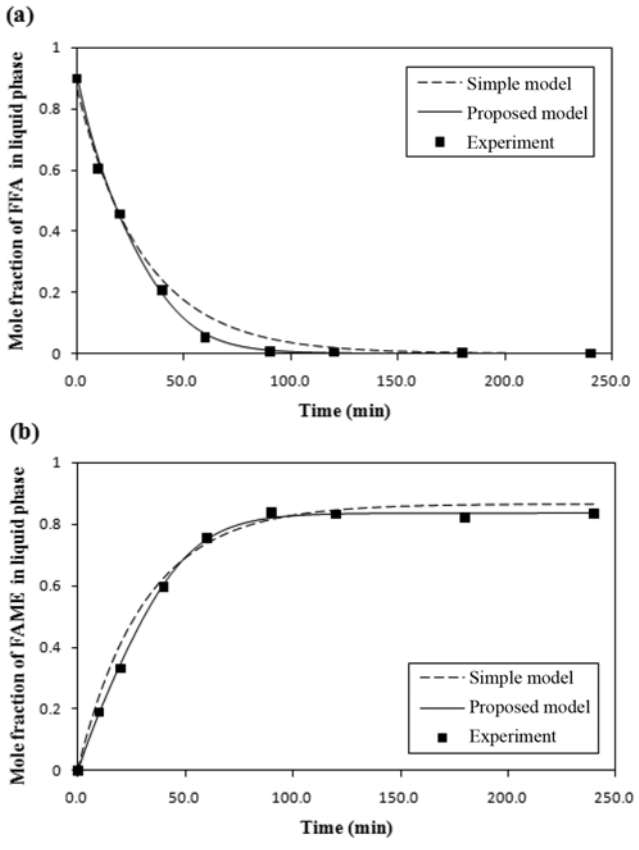


**Fig. 3. Mole fractions of (a) FFA and (b) FAME at 290 °C.**

as well as phase changes of water and methanol at high temperatures. In other words, the proposed model takes into account effects of evaporation of water and methanol at given temperature and pressure to provide more accurate description of experimental results. The evaporation is regarded as interfacial diffusion which is represented by Eq. (13) based on Fick's law.

$$J_i = Ac_{T,L}\left(\frac{D}{\sigma}\right)(x_i - x_i^{eq}) = Ac_{T,L}\nu_i(x_i - x_i^{eq}), \quad (i = M, W) \tag{13}$$

where D is the diffusion coefficient and $\sigma$ denotes a hypothetical distance required in the evaporation at the interface between vapor and liquid phase. It is very difficult to compute or to get values of the diffusion coefficient and the distance from the interface experimentally. In this study we selected a hypothetical interfacial diffusion rate ($\nu$, [cm/min]). We assumed that both the total number of moles of the liquid phase ($c_{T,1}$) and the interfacial area (A) can be regarded as constant. Now we can compute mole fractions of components in the liquid phase which is at equilibrium with the vapor phase as represented by Eq. (14).

$$\phi_i(T, P, y_i)Py_i = \gamma_i(T, x_i)P_i^{sat}x_i^{eq} \tag{14}$$

where $\gamma_i$ and $\phi_i$ denote the activity coefficient and the fugacity, respectively. At a given temperature and pressure, these values are specified by compositions in liquid and vapor phases during the reaction. Peng-Robinson and UNIQUAC models were used to calculate fugacity and activity coefficients, respectively. The saturation vapor pressure ($P_i^{sat}$) was estimated by Antoine's equation. While the reaction proceeds, diffusion occurs in the liquid phase to reach the equilibrium state with corresponding liquid mole fractions (see Eq. (14)). If the ideal liquid mole fractions at the equilibrium state are larger than actual mole fractions of the liquid phase, dissolution of components from the vapor phase to the liquid phase occurs. On the contrary, if the ideal liquid mole fractions at the equilibrium state are smaller than actual mole fractions of the liquid phase, evaporation of components from the liquid phase to the vapor phase occurs. In short, the driving force of the interfacial diffusion originates from the differences in mole fractions of water or methanol in liquid phase and ideal mole fractions at the equilibrium state.

Note that the reaction temperature in experiments is greater than the critical temperature of methanol ($T_c$=512.6 K). At this high temperature, methanol may exist as a single phase (i.e., gas phase) and it is not reasonable to use the phase equilibrium relation (14). Instead, the equilibrium liquid phase mole fraction of methanol may be set to zero, which means that there is no liquid methanol at equilibrium state. In our experiments the lowest reaction temperature tested is 230 °C (503.15 K), which is close to the critical temperature of methanol, and thus we can roughly assume that the equilibrium liquid phase mole fraction of methanol is equal to zero.

In the modeling we need to identify kinetic parameters such as $k_f$, $k_r$, $\nu_M$ and $\nu_W$. But it is difficult to determine the values of these kinetic parameters without additional experiments. Moreover, we could not find any reliable relationships between temperature and interfacial diffusion rates. So we employed a nonlinear programming scheme to estimate "optimal" parameter values which minimize the objective function given by Eq. (15).

$$F = \sum_t \sum_i w_i(x_{i,exp} - x_{i,cal})^2 \tag{15}$$

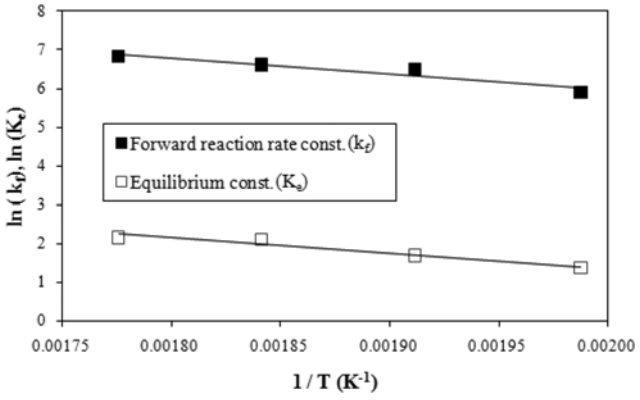


**Fig. 4. Arrhenius-van't Hoff plot.**

**Table 1. Kinetic parameters for forward reaction rate and equilibrium constants**

| | ln (pre-exponential factor) ($k_{f0}/K_{eq0}$) | Activation energy ($E_a$)/ heat of reaction ($\Delta H_R$) (kJ/mol) |
|---|---|---|
| $k_f$ | 14.29 | 34.67 |
| $K_{eq}$ | 9.30 | 33.03 |

where $w_i$ denotes weighting value for the component i. By using numerical values including interfacial diffusion rates of both methanol and water, we can determine the optimal reaction rate and equilibrium constants which minimize the objection function at each temperature. The equilibrium constant can be given by Eq. (16).

$$K_{eq} = \frac{k_f}{k_r} \tag{16}$$

From the Arrhenius-van't Hoff plot (Fig. 4) represented as the function of reaction temperatures, we can find the apparent activation energy and heat of reaction based on the intersection and the gradient obtained from the plot. Results are summarized in Table 1. Both the reaction rate constant and the equilibrium constant can be represented as functions of temperatures by applying the resultant numerical values to Arrhenius-van't Hoff equations given by Eq. (17) and (18).

$$k_f = k_{f0}\exp\left(\frac{E_a}{RT}\right) \tag{17}$$

$$K_{eq} = K_{eq,0}\exp\left(\frac{\Delta H_R}{RT}\right) \tag{18}$$

The next step is to employ the nonlinear programming scheme again to obtain "optimal" values for interfacial diffusion rates of water and methanol which minimize the objective function given by Eq. (15). The resultant values are shown in Fig. 5. It is well known that, as the temperature increases, the kinetic energy of a molecule increases to enhance the diffusion rate. This fact is well demonstrated in Fig. 5. Now we can perform numerical integrations of Eq. (3)-(10) by applying both reaction kinetic parameters and interfacial diffusion rates obtained from the nonlinear optimization.

Results of computations are displayed in Fig. 6 as well as experimental data for the purpose of comparison. In Fig. 6, changes in the

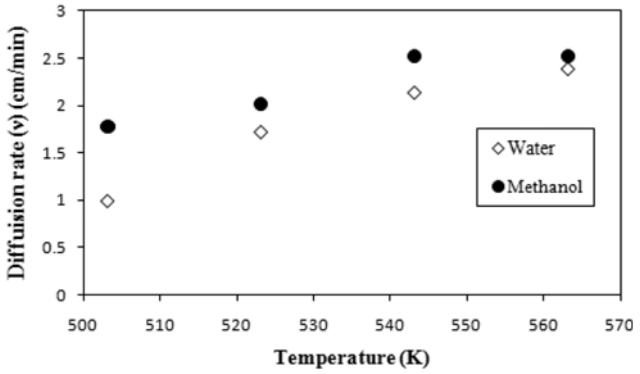


**Fig. 5. Optimized value for interfacial diffusion rates of water and methanol.**

liquid phase mole fractions with respect to reaction time are shown. Fig. 6 demonstrates that we can predict accurately the concentration profile of key components by using the proposed model. The performance of prediction for FFA and FAME appears to be better than that for water and methanol. Some errors in the values of inlet and exhaust flow rates may be expected during the cooling process of water and methanol prior to the measurement of liquid phase concentration, which seem to cause a little discrepancy in the behavior of water and methanol (see Fig. 6). Especially, for methanol, there was significant discrepancy between the experimental data and results of simulations during the first 50 minutes. As shown in Fig. 1, the methanol feed inlet located at the bottom of the reactor is very close to the outlet for sampling. Because of this configuration, measurement may be performed even before the injected methanol is mixed uniformly with liquid in the reactor. For this reason, the measured methanol concentrations are in general larger than those computed from the proposed model. Based on these observations, we arbitrarily set the weighting parameters for water and methanol to be 1 and those for FFA and FAME to be 10. In some sense, the weighting parameters may be regarded as "tuning" parameters in the proposed model. It is interesting that the differences between the experimental data and numerical simulation results decrease with increase of the reaction temperature. This fact is also apparent in Table 2 which shows values of RMSE at various reaction temperatures. The reason for decreasing discrepancy may be the formation of the homogeneous liquid phase due to the activated meth-

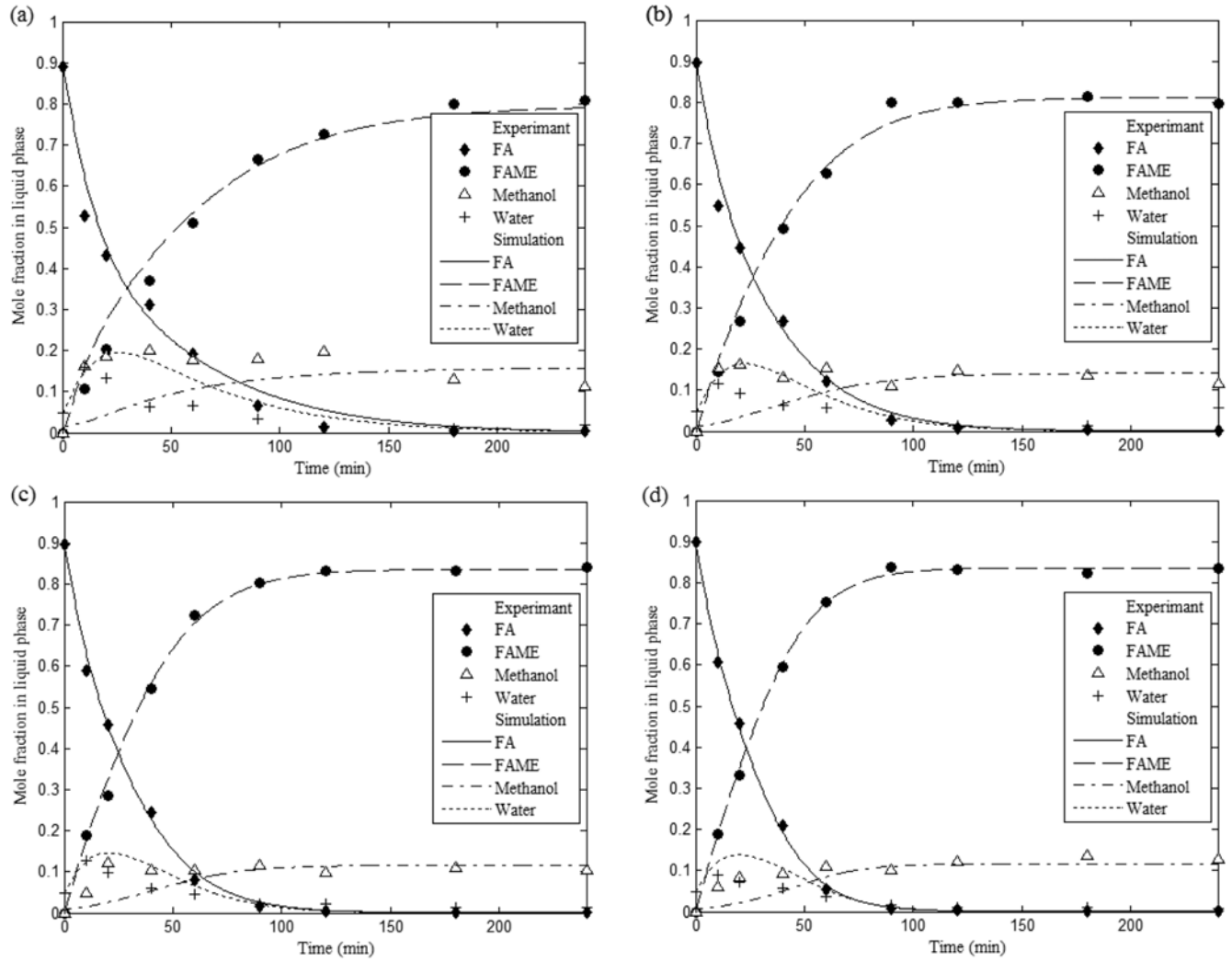


**Fig. 6. Mole fractions of key components in liquid phase at (a) 230 °C, (b) 250 °C, (c) 270 °C, (d) 290 °C (to be continued).**

**Table 2. Root mean square errors (RMSE) in the mole fraction of FFA and FAME**

| Temperature (°C) | Simple model | Proposed model |
|---|---|---|
| 230 | 0.295419 | 0.162929 |
| 250 | 0.208071 | 0.114308 |
| 270 | 0.158706 | 0.074579 |
| 290 | 0.153824 | 0.046151 |

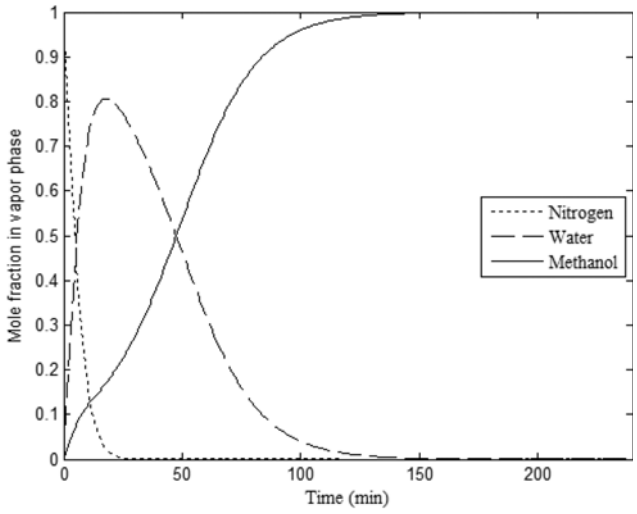


**Fig. 7. Dynamics of mole fractions in vapor phase at 290 °C.**

anol diffusion at higher temperatures. In fact, as the reaction temperature increases, the consumption of the methanol in the liquid phase is accelerated and the molecular kinetic energy increases to cause increase of the diffusion rate of the methanol fed into the reactor.

Fig. 7 shows changes of mole fractions in the vapor phase with respect to reaction time at 290 °C. As the reaction proceeds, the inert nitrogen gas is pushed out by a significant amount of steam generated by the evaporation of water caused by the esterification reaction between FFA and methanol. Moreover, as the acid concentration decreases, the formation rate of water decreases while the evaporation rate of the methanol not consumed by the reaction increases to occupy the major portion of the vapor phase.

## CONCLUSIONS

We investigate the biodiesel production reaction performed in a semi-batch reactor at 230-290 °C and 8.5 bar both experimentally and theoretically. The reaction conditions are relatively lower than those employed in the reaction using supercritical methanol. For the modeling of the reaction, we employed a nonlinear programming scheme to estimate reaction kinetic parameters which minimize a specified objective function. As the reaction temperature increases, the consumption of the methanol in the liquid phase is accelerated and the molecular kinetic energy increases to cause increase of the diffusion rate of the methanol fed into the reactor. Imperfect mixing in the liquid phase at the initial reaction stage causes a little discrepancy between the experimental data and results of simulations. Overall, the proposed model represents the biodiesel production reaction effectively.

## ACKNOWLEDGEMENT

This work is the outcome of a Manpower Development Program for Energy & Resources supported by the Ministry of Knowledge and Economy (MKE).

## NOMENCLATURE

A : surface area between liquid phase and vapor phase [$cm^2$]
$C_i$ : concentration of component i in the liquid phase [$mol/cm^3$]
D : diffusion coefficient [$cm^2/min$]
$E_a$ : apparent activation energy [kJ/mol]
F : objective function indicating differences in estimated and experiment data
$F_L$ : molar liquid feed flow rate of methanol [mol/min]
$F_V$ : molar vapor flow rate from reactor to atmosphere [mol/min]
$\Delta H_R$ : heat of reaction [kJ/mol]
$J_i$ : molar diffusion flow rate from liquid phase to vapor phase [mol/min]
$k_f$, $k_r$ : forward and reverse reaction rate constants [$cm^3/mol \cdot min$]
$K_{eq}$ : equilibrium constants
MW : molecular weight [g/mol]
$n_{i,p}$ : moles of the component i in the phase p (liquid or vapor) [mol]
P : pressure [bar]
$P^{sat}$ : saturated vapor pressure [bar]
R : gas constant [kJ/mol·K]
$r_i$ : reaction rate [mol/min]
T : temperature [K]
t : evolution time [min]
V : volume [$cm^3$]
$w_i$ : weighting value
$x_i$ : mole fraction of component i in liquid phase
$x_i^{eq}$ : equilibrium mole fractions of component i in liquid phase
$y_i$ : mole fraction of component i in vapor phase
$\gamma_i$ : activity coefficient
$\rho_i$ : density of component i [$g/cm^3$]
$\sigma_i$ : hypothetical distance required to evaporation [cm]

**Subscripts**

0 : pre-exponential factor
A : free fatty acid (FFA)
cal : computed value
E : fatty acid methyl ester (FAME)
exp : experimental data
L : liquid phase
M : methanol
$N_2$ : nitrogen
i : component i (i=FFA, FAME, methanol, water)
T : total components in the same phase
V : vapor phase
W : water

## REFERENCES

1. R. Tesser, M. Di Serio, M. Guida, M. Nastasi and E. Santacesaria, *Ind. Eng. Res.*, **44**, 7978 (2005).

2. S. Zallaikah, C. Lai, S. R. Vali and Y. H. Ju, *Bioresour. Technol.*, **96**, 1889 (2005).
3. A. Petchmala, N. Laosiripojana, B. Jongsomjit, M. Goto, J. Panpranot, O. Mekasuwandumrong and A. Shotipruk, *Fuel*, **89**(9), 2387 (2010).
4. Y.-W. Lee, E.-S. Song and H. Kim., *Clean Technol.*, **11**(4), 171 (2005).
5. M. Diasakou, A. Louloudi and N. Papayannakos, *Fuel*, **77**(12), 1297 (1998).
6. Joelianingsih, H. Nabetani, S. Hagiwara, Y. Sagara, T. H. Soerawidjaya, A. H. Tambunan and K. Abdullah, *J. Chem. Eng. Japan*, **40**(9), 780 (2007).
7. M. Berrios, J. Siles, M. A. Martin and A. Martin., *Fuel*, **86**, 2383 (2007).
8. E. Santacesaria, R. Tesser, M. Di Serio, M. Guida, D. Gaetano, A. G Agreda and F. Cammarota, *Ind. Eng. Res.*, **46**, 8355 (2007).